Finite element simulation of composite reinforcement draping using a three node semi discrete triangle

N. Hamila[1], P. Boisse[1], S. Chatel[2]

[1]*INSA de Lyon, LaMCoS – 20 avenue Einstein, 69621 Villeurbanne, France.*
URL: lamcos.insa-lyon.fr/ e-mail: nahiene.hamila@insa-lyon.fr; philippe.boisse@insa-lyon.fr

[2]*EADS France - 12 rue Pasteur, 92152 Suresnes, France.*
URL: www.eads.com e-mail: sylvain.chatel@eads.net

ABSTRACT: Continuous and discrete approaches for forming simulations of textile performs both involve difficulties and drawbacks. The semi-discrete method is an alternative based on a meso-macro approach. It is based on specific finite elements made of a discrete number of the components of the textile at lower scale. Their strain energy in the interpolated displacement field leads to the nodal interior loads of the element. In this paper a new three node element is proposed. It is made up of warp and weft fibres, the tensile and in plane shear energy of which are considered. The directions of the warp and weft yarns are arbitrary with regard to the element sides. That is very important in case of simultaneous multiply draping simulations and when using remeshing. The determination of the material data necessary to the simulation from standard tensile and bias tests is straightforward. A set of elementary tests and mono and multi-ply draping shows the efficiency of the approach.

Key words: Instructions Fabrics/textiles, Composites, Forming, Finite element, Meso-macro.

1 INTRODUCTION

The increase in the usage of textile composites, especially in aeronautic applications, due to their high mechanical properties leads to develop adequate design and analysis methods and especially validated simulation tools in this domain (for instance the European project ITOOL : Integrated tool for simulation of textile composites [1]).
Among the different codes developed in this framework, draping simulation plays a large part. First, the simulation can give the conditions (for instance loads on the tools, initial orientation, type of material etc) that will make the forming of the textile reinforcement possible, and also describe possible defects after forming (wrinkles, porosities, yarn fractures etc). Secondly, and unique to composite forming analysis, is the need to know at any point the directions and density of the fibres after forming. These directions and densities are very important for analyzing how the composite part will behave in use, with regards to stiffness, damage, fatigue etc [2]. They also strongly influence the permeability of the textile reinforcement and must be taken into account in case of LCM Processes [3].
For a physical (or mechanical) analysis of a composite forming process, the complete model must include all the equations for the mechanics, especially equilibrium, constitutive equations, and boundary conditions. These equations must be solved numerically, with some approximations. Finite Element analysis of the composite forming process includes modelling the tools, the contact and friction between the different parts, and above all, the mechanical behaviour of the composite during forming [4].

2 SPECIFIC MECHANICAL BEHAVIOR

2.1 Tension and in plane shear

The mechanical behaviour of textiles used as reinforcement for composites is very specific [5-9]. During a forming process, there is no matrix (first stage of the RTM process for instance) or the resin is very weak and play a second order role. The textile

composite reinforcements are made of fibres (usually carbon, glass or aramid), the diameter of which is very small (5 to 7 µm for carbon, 10-20 µm for aramid, 5-25 µm for glass). Consequently these fibres can only be submitted to tensile loads in the fibre direction. The assembly of yarns (or fibres) in fabrics, NCF (Non Crimp Fabrics), knitted or braided materials leads to different mechanical properties of the resulting textile material, but the tensile stiffness in the fibre directions remain the most important. Nevertheless, for some types of analysis, it can be necessary to take the second order rigidities into account because those play a significant role. For instance, it has been shown that the in-plane shear stiffness play a main role in wrinkle development in draping simulations when the shear angle become large [10]. In the present work, tensile and in plane shear rigidities and corresponding strain energies will be considered.

2.2 Simplified dynamic equation

The textile composite reinforcement under consideration has two fibres directions (warp and weft). It can be a woven textile or a biaxial NCF (Non-Crimp Fabric) (Figure1). Material coordinates r^1 and r^2 along warp and weft fibre directions define the material covariant vectors $\underline{k}_1$ and $\underline{k}_2$ (Figure 1):

$$\underline{k}_1 = \frac{\partial \underline{x}}{\partial r^1} \qquad \underline{k}_2 = \frac{\partial \underline{x}}{\partial r^2} \tag{1}$$

For a fibre in direction $\underline{k}_1$, the tension on a fibre is defined by :

$$\underline{\underline{T}} = T^{11}\, \underline{k}_1 \otimes \underline{k}_1 \tag{2}$$

where $T^{11} = \int_{S_1} \sigma^{11} dS$, $\underline{\underline{\sigma}}$ is the tensile Cauchy stress tensor ($\underline{\underline{\sigma}} = \sigma^{11}\, \underline{k}_1 \otimes \underline{k}_1$), and S is the section of the fibre.

In the same way for a fibre in direction $\underline{k}_2$:

$$\underline{\underline{T}} = T^{22}\, \underline{k}_2 \otimes \underline{k}_2 \tag{3}$$

where $T^{22} = \int_{S_2} \sigma^{22} dS$ and $\underline{\underline{\sigma}} = \sigma^{22}\, \underline{k}_2 \otimes \underline{k}_2$

Considering a textile unit cell submitted to in plane shear strain such as shown figure 1, the warp fibres exert loads on weft fibres that can be due to weaving or to stitching in case of NCF. Their resultant is a shear torque C_s.

Taking these definitions and assumptions into account, the work of the interior load in a virtual displacement field $\underline{\eta}$ takes the following form. :

$$W_{int}(\underline{\eta}) = \sum_{p=1}^{nwa} \int_{{}^{p}l} {}^{p}T^{11}\, {}^{p}\varepsilon_{11}(\underline{\eta})\, dl + \sum_{p=1}^{nwe} \int_{{}^{p}l} {}^{p}T^{22}\, {}^{p}\varepsilon_{22}(\underline{\eta})\, dl + \sum_{q=1}^{ncell} {}^{q}C_s\, {}^{q}\gamma(\underline{\eta}) \tag{4}$$

where nwa and nwe are the number of warp and weft fibres in the domain under consideration Ω, ncell is the number of unit cells. $\varepsilon_{\alpha\alpha}$ are the axial components of the symmetrical gradient of the virtual displacement (α and β are indexes taking values 1 and 2):

$$\underline{\underline{\nabla^s}}(\underline{\eta}) = \varepsilon_{\alpha\beta}(\underline{\eta})\, \underline{k}^{\alpha} \otimes \underline{k}^{\beta} \tag{5}$$

$\underline{k}^1$, $\underline{k}^2$ are the contravaiant vectors associated to $\underline{k}_1$, $\underline{k}_2$ and such as $\underline{k}_\alpha . \underline{k}^\beta = \delta_\alpha{}^\beta$.

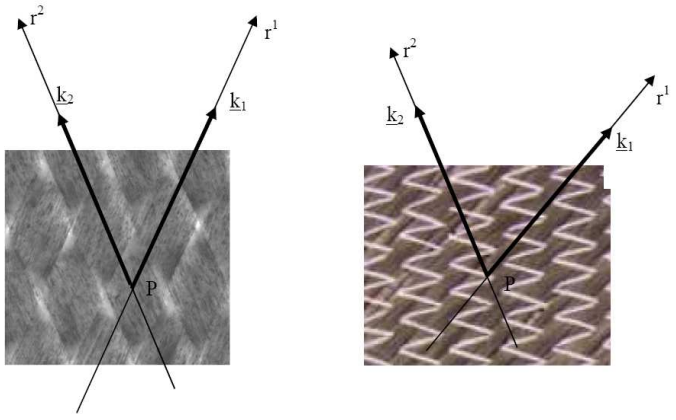

Fig. 1. Material coordinates along the fibre directions and associated material vectors

$\gamma(\underline{\eta})$ is the variation of angle between warp and weft yarns in the virtual displacement field.

The form (4) of the virtual work of interior loads leads to a simplified dynamic equation that will be used in a dynamic explicit approach :

$$\sum_{p=1}^{nwa} \int_{{}^{p}l} {}^{p}T^{11}\, {}^{p}\varepsilon_{11}(\underline{\eta})\, dl + \sum_{p=1}^{nwe} \int_{{}^{p}l} {}^{p}T^{22}\, {}^{p}\varepsilon_{22}(\underline{\eta})\, dl + \sum_{q=1}^{ncell} {}^{q}C_s\, {}^{q}\gamma(\underline{\eta}) - W_{ext}(\underline{\eta}) = -\int_{\Omega} \rho\, \underline{\ddot{u}} . \underline{\eta}\, dV \tag{6}$$

$$\forall \underline{\eta} / \underline{\eta} = 0 \text{ on } \Gamma_u$$

$\underline{\ddot{u}}$ is the acceleration of the point P, ρ is the mass per volume.

In this dynamic equation, the quantities are not those of continuum approaches. We have seen that those are delicate for fibrous material at large strains especially because quantities such as stresses are not well defined and because the continuity of the displacement field with the fibrous material is not clear. In equations (4)(6) the quantities such as tensions in a fibre and the torque due to the shear of

a set of warp fibres on weft ones within a unit cell, are clearly defined and simple. We shall speak for this approach and for the finite element developed further of semi-discrete approach. The domain or element is not a continuum. It is composed of fibres in tension and shear.

3 SEMI-DISCRETE THREE NODE FINITE ELEMENT

3.1 Tensile elementary nodal interior load

Taking the form of the virtual displacement gradient into account :

$$\underline{\underline{\nabla^s}}(\underline{\eta}) = \varepsilon_{\alpha\beta}(\underline{\eta})\ \underline{k}^{\alpha} \otimes \underline{k}^{\beta} = \frac{1}{2}\left(\frac{\partial \underline{\eta}}{\partial r^{\alpha}} \cdot \underline{k}_{\beta} + \frac{\partial \underline{\eta}}{\partial r^{\beta}} \cdot \underline{k}_{\alpha}\right)\underline{k}^{\alpha} \otimes \underline{k}^{\beta} \tag{7}$$

the elementary tensile virtual work can be written :

$$W_{int}^{et}(\underline{\eta}) = \sum_{p=1}^{nwae} \int_{p_1}^{p} {}^{p}T^{11} \left(\frac{\partial \underline{\eta}}{\partial r^{1}} \cdot \underline{k}_1\right) dl + \sum_{p=1}^{nwee} \int_{p_1}^{p} {}^{p}T^{22} \left(\frac{\partial \underline{\eta}}{\partial r^{2}} \cdot \underline{k}_2\right) dl = W_{int}^{etwa}(\underline{\eta}) + W_{int}^{etwe}(\underline{\eta}) \tag{8}$$

where nwae et nwee are the number of fibres in warp and weft directions in the element

Because of the linear interpolation, the strain interpolation terms B_{1ij} are very simple and constants in the element. The strains and consequently the tensions are constant in the element:

$$\left(F_{int}^{etwa}\right)_{ij} = \frac{1}{2}\left\|\underline{k}_1\right\| nwae\, B_{1ij} T^{11} \tag{9}$$

In the same way in the weft direction :

$$\left(F_{int}^{etwe}\right)_{ij} = \frac{1}{2}\left\|\underline{k}_2\right\| nwee\, B_{2ij} T^{22} \tag{10}$$

3.2 In plane shear nodal interior loads

In this section, the in plane shear interior load vector due to in plane shear $\mathbf{F}_{int}^{es}$ (equation 11) is calculated in function of the shear torque resulting of actions of warp yarns on weft yarns in a unit cell and of shear strain interpolation.

$$W_{int}^{es}(\underline{\eta}) = \sum_{q=1}^{ncell} {}^{q}C_s\ {}^{q}\gamma(\underline{\eta}) = \boldsymbol{\eta}_n^{T}\mathbf{F}_{int}^{es} \tag{11}$$

The virtual shear angle $\gamma(\underline{\eta})$ (variation of angle between warp and weft directions) in the virtual displacement $\underline{\eta}$ is given by the gradient of $\underline{\eta}$ [10]:

$$\gamma(\underline{\eta}) = \left(\underline{\underline{\nabla\eta}} \cdot \frac{\underline{k}_1}{\left\|\underline{k}_1\right\|}\right) \cdot \frac{\underline{k}^2}{\left\|\underline{k}^2\right\|} + \left(\underline{\underline{\nabla\eta}} \cdot \frac{\underline{k}_2}{\left\|\underline{k}_2\right\|}\right) \cdot \frac{\underline{k}^1}{\left\|\underline{k}^1\right\|} \tag{12}$$

As it has been done in equation (26), accounting for the interpolation in the triangle, the components of the gradient of $\underline{\eta}$ can be expressed in function of the components of the virtual displacement η_{ij}. Consequently :

$$\gamma(\underline{\eta}) = \left(B_{1ij} \frac{\underline{k}^1}{\left\|\underline{k}_1\right\|} \cdot \frac{\underline{k}^2}{\left\|\underline{k}^2\right\|} + B_{3ij} \frac{\left\|\underline{k}^2\right\|}{\left\|\underline{k}_1\right\|}\right)\eta_{ij} + \left(B_{4ij} \frac{\left\|\underline{k}^1\right\|}{\left\|\underline{k}_2\right\|} + B_{2ij} \frac{\underline{k}^2}{\left\|\underline{k}_2\right\|} \cdot \frac{\underline{k}^1}{\left\|\underline{k}^1\right\|}\right)\eta_{ij} = B_{\gamma ij}\eta_{ij} \tag{13}$$

The nodal interpolation of $\gamma(\underline{\eta})$ is known. $B_{\gamma i1}$ is constant in the triangle finite element, therefore:

$$\left(F_{int}^{es}\right)_{ij} = ncell\, B_{\gamma ij} C_s \tag{14}$$

4 NUMERICAL TESTS

4.1 Single ply forming

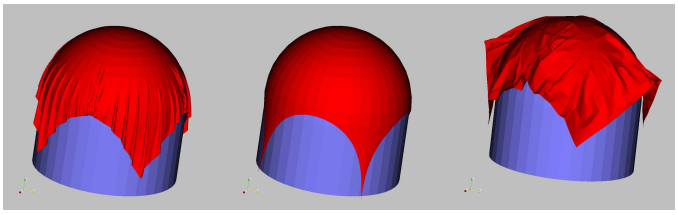

Fig. 2. Draping on a dome. (a) woven shear stiffness (b) without shear stiffness (c) isotropic shear stiffness

An initially flat square fabric is draped on a dome (figure 2). The mesh is made of 2×100×100 triangles). The yarns are parallel to the sides of the square fabric. Three different behaviours are considered for the woven reinforcement. In figure 2a the tensile and shear behaviour presented above in the present paper is used. The draped shape is correct. The membrane assumption (the element does not involves any bending stiffness) leads to wrinkles that are numerous in the corners but that are small. Some bending stiffness would increase the size of the wrinkles and decrease their number. In figure 2b, the shear stiffness is neglected. The draping is easily obtained but there is no wrinkle because the shear angle can be infinitely large in the corners of the sheet. This solution is close to those that would be obtained by a fishnet algorithm that appears to be unsuitable in this case.

In figure 2c, an isotropic behaviour is used for the sheet. For instance it could be a paper sheet. The

draping is not possible. The required large shear angles in the corners are not allowed by this behaviour. That show the very important role of the in plane shear behaviour in draping/forming of membrane. A textile can be shaped on a double curved surface because there are possible large rotations between warp and weft fibres and in plane shear stiffness is weak. In the case of an isotropic membrane that is not possible. On the other hand the shear stiffness that increases when the shear angle becomes large leads to wrinkles. If this shear stiffness is neglected there will be no wrinkle in any case.

4.2 Simultaneous forming of three plies

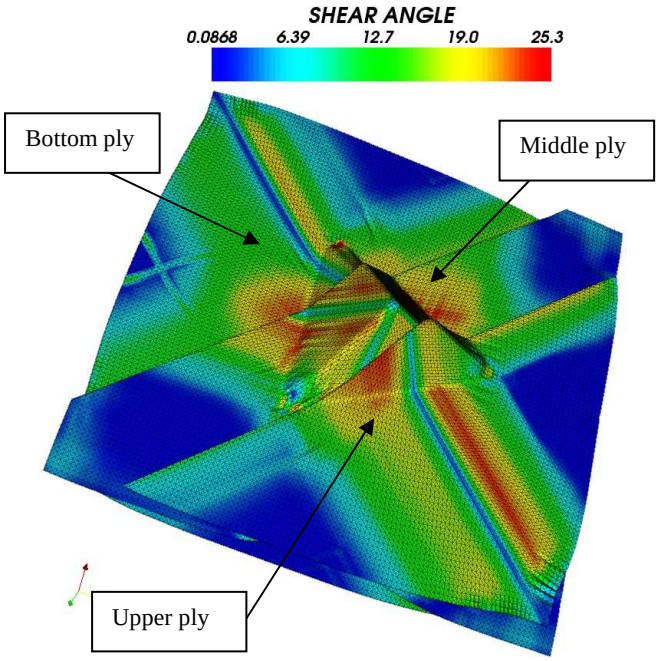

Fig. 3. Simultaneous forming of three plies

The tetrahedral forming is performed simultaneously for three plies. It corresponds to the experiments performed in LMSP Orleans [11]. The superior and inferior plies are oriented at ±45° while the middle ply is oriented at 0-90°. The mesh is the same for each ply. Figure 3 show the shear angle γ in the different plies. The solution depends on the friction between the plies which is an important point for multiply forming [12].

5 CONCLUSION

This semi-discrete approach avoids the difficulty of the determination of an equivalent continuous mechanical behaviour which in case of fibrous material at large strain has proved to be very difficult. It also reduces the size of the computations in comparison to discrete approaches.

Bending stiffness is actually very small for most textile fabrics. It can modify the wrinkling shape. It will be interesting to associate the semi-discrete membrane approach developed in the present paper to bending stiffness such as taken into account in three node plate or shell elements. The bending rigidity will have to be very specific to textile material. Then it will be possible to analyse its influence and in which case it is necessary.

REFERENCES

1. ITOOL ‘Integrated Tool for Simulation of Textile Composites’, European Specific Targeted, Research Project, SIXTH FRAMEWORK PROGRAMME, Aeronautics and Space, http://www.itool.eu
2. Potluri P., Parlak I., Ramgulam R., Sagar T.V., Analysis of tow deformations in textile preforms subjected to forming forces, Composites Science and Technology, 2006, 66, 297–305
3. Bickerton S., Simacek P. Guglielmi S.E., Advani S.G., Investigation of draping and its effects on the mold filling process during manufacturing of a compound curved composite part. Composite Part A, 1997, 28, 801-816
4. Boisse P. Finite element analysis of composite forming. In: Long AC, editor. Composite forming technologies. Woodhead Publishing, 2007. Chapter 3: p.46-79.
5. Scardino F. An introduction to textile structures and their behaviour, Textile structural composites. In: Chou T.W and Ko F.K., editor. Composite Material Series, Elsevier, 1989; p 1-26
6. Long A.C., Clifford M.J. Composite forming mechanisms and material characterisation. In: Composites Forming Technologies. Woodhead Publishing, 2007. p. 1, 21.
7. Lomov, S. V., Huysmans, G., Luo, Y., Parnas, R., Prodromou, A., Verpoest, I., Phelan, F. R. Textile Composites Models: Integrating Strategies. Composites part A, 2001; 32(10):1379-1394
8. Peng X., Cao J. : A continuum mechanics-based non-orthogonal constitutive model for woven composite fabrics. Composites Part A, **36**, 859–874 (2005)
9. Boisse P., Zouari B., Daniel J. L., Importance of In-Plane Shear Rigidity in Finite Element Analyses of Woven Fabric Composite Preforming. Composites A. 2006; 37(12): 2201-2212.
10. Hamila N., Boisse P., Simulations of textile composite reinforcement draping using a new semi-discret three node finite element. Composites B. 2007; doi:10.1016/j.compositesb.2007.11.008
11. Allaoui S., Launay J., Soulat D., Chatel S. Experimental tool of woven reinforcement forming. ESAFORM 2008 Proceeding.
12. Gorczyca J., Sherwood J., Chen J. A friction model for thermostamping commingled glass–polypropylene woven fabrics. Composites: Part A, 2007; 38:393–406.